Nonequilibrium Landau-Zener tunneling in exciton-polariton condensates

Xingran Xu,[1,2,3] Zhidong Zhang,[2,3] and Zhaoxin Liang[1,*]

[1] *Department of Physics, Zhejiang Normal University, Jinhua, 321004, China*

[2] *Shenyang National Laboratory for Materials Science, Institute of Metal Research, Chinese Academy of Sciences, Shenyang, 110016, China*

[3] *School of Materials Science and Engineering, University of Science and Technology of China, Hefei, 230026, China*

(Received 4 December 2019; revised 19 August 2020; accepted 19 August 2020; published 11 September 2020)

For describing a coherent quantum two-level system driven by a linearly time-dependent energy separation of the diabatic states, the Landau-Zener model is routine to serve as a textbook model for its dynamics. Along this research line, a particularly intriguing question is whether the framework of Landau-Zener theory can be extended to an intrinsically nonequilibrium quantum system with coherent and dissipative dynamics occurring on an equal footing. In this work, we are motivated to investigate the Landau-Zener problem of polariton condensates in a periodic potential under nonresonant pumping by using the driven-dissipative Gross-Pitaevskii equations coupled to the rate equation. Within the two-mode approximation, a nonequilibrium Landau-Zener model, characterized by coherent and dissipative dynamics occurring on an equal footing, is derived. Fundamentally different from the previous Landau-Zener model, the total density of nonequilibrium Landau-Zener model, in general, is not the conserved quantity anymore due to the dissipative nature. In a surprise, the parameter regimes of the total density still being conserved can still be found. The motion of Hamiltonian of the nonequilibrium Landau-Zener problem in phase space is further discussed. The instability of the band structure can also be studied by the curvatures in phase space, and there may be two loops in the middle of the Brillouin zone. Detailed analysis of the nonequilibrium nature on the tunneling rate will open a new perspective toward understanding the Landau-Zener problem.

DOI: 10.1103/PhysRevA.102.033317

I. INTRODUCTION

Adiabatic transitions at avoided level crossings play an essential role in many dynamical processes with potential applications of the quantum state preparation [1]. The paradigmatic model studying adiabatic transitions is referred to as the Landau-Zener (LZ) problem [2,3]. In more details, the dynamics of the model system are restricted to two quantum states coupled with a constant tunneling matrix element. A control parameter is swept through the avoided level crossing at a constant velocity. The focus of the LZ problem is on the final occupation probability of the two states. The pure LZ problem was solved by Landau [2] and Zener [3] independently. Then, Wu and Niu [4,5] have extended the LZ model from the linear quantum system to nonlinear physical systems inspired by the experimental realization of an optically trapped ultracold Bose gas [6,7]. Along this research line, the purpose of the present work is further extension of the LZ theory to include an intrinsically nonequilibrium nature for a quantum system motivated by the experimental progress of exciton-polariton Bose-Einstein condensate (BEC) [8–12].

Exciton-polariton BEC, which can be achieved even at room temperature due to the exceedingly light effective mass, has the crucial novelty of being an intrinsically nonequilibrium system with coherent and dissipative dynamics occurring on an equal footing [8–12]. Up to now, there are lots of work discussing the steady states and elementary excitations of polaritons in both one- and two-component condensates theoretically [13–20] and experimentally [21–24]. Meanwhile, nonlinear phenomena like oblique dark solitons, vortices, bright solitons [25–27], and dark-bright solitons [28–33] in a polariton condensate are the current hot topics. Besides, tuning the interaction of polaritons has been demonstrated by using biexcitonic Feshbach resonance in recent experiments [34,35]. Moreover, spontaneous oscillations in a microcavity polariton bosonic Josephson junction with strong imbalance of the population in a double well [36–39] has inspired the ongoing interests in investigating a polariton condensate in a periodic potential.

Experimentally, the periodic potential in polariton can be realized by surface acoustic wave (SAW) and buried mesa array [40–44]. The band structure of a polariton condensate as a direct result of introducing a periodic potential appeals because it provides a natural dissipative quantum simulator for studying topological properties [45,46], e.g., spin Hall effects [47,48], the flat band in Lieb lattice [49–53]. With the state-of-the-art technologies of SAW, it's possible to trap a polariton BEC in a *moving* periodic potential [54]. A timely question arises to study adiabatic transitions of a polariton condensate around the edge of the Brillouin zone, i.e., the nonequilibrium LZ problem.

In this work, we are motivated to investigate the nonequilibrium LZ problems of a polariton BEC theoretically. First, at the mean-field level, an optically trapped polariton BEC can be well described by the dissipative Gross-Piteavskii (GP)

[*] zhxliang@gmail.com

equation coupled to a rate equation. Within the framework of the two-mode approximation, a nonequilibrium LZ model, characterized by coherent and dissipative dynamics occurring on an equal footing, is derived. Second, we investigate the steady states of the LZ model both numerically and analytically. Fundamentally from the equilibrium counterparts of the LZ model, the total particle number of the nonequilibrium LZ model is not conserved quantity any more in general. However, we still find three kinds of parameter regimes in which the total particle number of the dissipative system is still conversed by calculating $dn/dt = 0$. Next, we study the nonequilibrium LZ tunneling of the model system numerically. It's difficult to define a tunneling probability of a dissipative system with a nonconserved particle number. Here we choose to use the occupation of each state to describe this adiabatic process. We find fluctuation has a peak near $t = 0$, which leads to the atom loss and presents how the interaction affects the occupation after tunneling. Finally, we study the motion of the nonequilibrium LZ model in phase space. The imaginary part of the Hamiltonian is a periodic function along with the relative phase, while the real part can have a new result for adjustable condensate density. When the pumping rate is far beyond the threshold, there may be two crossovers in the middle of the Brillouin zone, as is famous for "swallowtails" [43].

The emphasis and value of the present work are to provide a theoretical model, i.e., an extended LZ model in describing the open quantum system with coherent and dissipative dynamics occurring on an equal footing capturing the key information of the nonequilibrium nature affecting adiabatic transitions at avoided level crossings. We remark that in the case of vanishing the dissipation parameters, our model can be simplified into the coherent model, which has been widely explored both theoretically and experimentally in the context of the ultracold quantum gas [4,5]. We hope the model adopted in this work can serve as a simple model to study adiabatic transitions at the avoided level crossing for a nonequilibrium quantum system.

The paper is organized as follows. In Sec. II, we introduce polariton in a periodic potential, which can be described by a dissipative GPE coupled to the rate equation of a reservoir under pumping. In Sec. III, we investigate the steady states of the model, both numerically and analytically, and simplify the problem into a two-level problem. In Sec. IV, we evolute the model from the lower level at $t = -\infty$ to study the LZ tunneling. In Sec. V, we transform the Hamiltonian into phase space to find the motion of fixed points under different pumping rates. In Sec. VI, we conclude with a summary of our main results and final remarks.

II. NONEQUILIBRIUM LANDAU-ZENER MODEL

Our goal is to investigate the nonequilibrium LZ problem of an exciton-polariton BEC characterized by coherent and dissipative dynamics occurring on an equal footing. To this end, we are interested in a nonresonant pumped exciton-polariton BEC in a periodic potential. Recently, several schemes of the periodic potential landscape engineering [40–44] have been proposed, e.g., utilizing metallo-photonic waveguides [55], using photonic crystal structures [56], or depositing a thin metal film [40,57]. Moreover, the almost free choice of the confinement strengths and trapping geometries have provided powerful means for control and manipulation of the polariton systems both in the semiclassical and quantum regimes [58]. In this work, we focus on that array of one-dimensional cigar-shaped exciton-polariton BEC trapped in an all-optically controlled dynamic lattice for polaritons working in the ultraviolet wavelength range at room temperature, where the optical lattice was realized on a one-dimensional (1D) ZnO microrod using an array of periodically arranged laser spots in a fully reconfigurable manner [59]. Theoretically, the order parameter for the condensate is described by a one-component time-dependent wave function ψ; the reservoir on the relevant time scales can be modeled by a scalar density denoted by n_R.

At the mean-field level, the dynamics of the order parameter for the polariton condensates in the accelerating lattice labeled by ψ can be well described by the driven-dissipative GP equation [8,13,14], i.e.,

$$i\hbar\frac{\partial}{\partial t}\psi = -\frac{1}{2m}\left(\hbar\frac{\partial}{\partial x} - i\alpha t\right)^2\psi + V_0\cos(k_L x)\psi + g|\psi|^2\psi + g_R n_R\psi + i\frac{\hbar}{2}(Rn_R - \gamma_C)\psi, \quad (1)$$

with m being the mass of the polariton, g the interaction constant, γ_C the decay rate of the polariton condensate, and g_R characterizing the interaction between the condensate and reservoir. V_0 in Eq. (1) is the strength of the periodic potential with the wave number of k_L that can be controlled with a spatial quantization energy modulation of either the photonic or excitonic component [44,60–62]. We emphasize that the purpose of this work is to provide the simplest theoretical nonequilibrium LZ model where the dissipative nature is captured by the incoherent reservoir n_R below rather than the imaginary part of periodic potential [60]. Therefore, we limit ourselves into the case of the imaginary part of periodic potential in Eq. (1) being zero although tuning strength of the periodic potential in this case remains experimentally challenging.

The term of $\alpha = ma_c$ in Eq. (1) can be regarded as the vector potential gauge, which can be realized experimentally due to the inertial force in the comoving frame of the accelerating lattice. Experimentally, the term of α in Eq. (1) can be experimentally realized in principle as follows. A one-dimensional optical lattice can be created by taking a linearly polarized laser beam and retro-reflecting it with a high-quality mirror [7,40,54]. Another phase-coherent laser beam is introduced to make a frequency shift $\Delta\nu_L$ between two lattice beams. The original lattice potential will become unstable and move at a velocity $\nu_{\rm lat} = d\Delta\nu_L$ where d is the lattice spacing. The BEC in the lattice will be accelerated with force $F = md\frac{d\Delta\nu_L}{dt}$ [7,54], corresponding to the term of $\alpha = ma_c$ in Eq. (1).

Equation (1) is coupled to an incoherent reservoir n_R, which is described by a rate equation [13,14], i.e.,

$$\frac{\partial}{\partial t}n_R = P - \gamma_R n_R - R|\psi|^2 n_R, \quad (2)$$

where P is an off-resonant continuous-wave pumping rate, γ_R is the dissipative rate of the reservoir, and R stands for the stimulated scattering rate of reservoir polaritons into the condensate. The reservoir is a dynamical variable, which can modify the dispersion of the condensate rather strongly. If the polariton distribution in the reservoir region and all coherences between the reservoir and the condensate relax on a short time scale as compared to the condensate dynamics, the state of the reservoir is fully determined by its local density [13].

Before investigating the nonequilibrium LZ problem, we first briefly review some important features of a polariton condensate in the uniform space [13], corresponding to the vanishing of both the periodic potential and the gauge potential, i.e., $V_0 = 0$ and $\alpha = 0$ in Eq. (1). There, the steady-state under a continuous-wave and uniform pumping can be obtained as $\psi_0 = \sqrt{n_0}e^{-i(gn_0+g_Rn_R^0)t/\hbar}$ and $n_R^0 = \gamma_C/R$ with $n_0 = (P - P_{\rm th})/\gamma_C$ and $P_{\rm th} = \gamma_R\gamma_C/R$.

In the presence of periodic lattice potentials and the gauge potential, i.e., $V_0 \neq 0$ and $\alpha \neq 0$ in Eq. (1), there will exist the band structure in the polariton condensate, where the longest lifetime characterizes the lowest-band top state. The tunneling mainly occurs around the edge of the Brillouin zone, so we are motivated to project Eqs. (1) and (2) into the plane wave two-mode basis in the neighborhood of the Brillouin zone edge of $k = \frac{1}{2}$ and search for the solutions of Eqs. (1) and (2) in the form,

$$\psi(x,t) = a(t)e^{ikx} + b(t)e^{i(k-k_L)x}, \tag{3}$$

$$n_R(x,t) = n_R^0 + 2u(t)\cos(k_Lx), \tag{4}$$

with the reservoir density of $n_R(x,t)$ having a periodic fluctuation described by the $u(t)$ term in Eq. (4). In principle, the fluctuation of the reservoir should be written as $\sum_n u_n(t)e^{inx}$, however, we just take $n = 0, \pm 1$ within the framework of the two-mode approximation. We remark that Eqs. (3) and (4) can be deduced into the corresponding results of Ref. [62] without considering the reservoir density's fluctuation by taking $u = 0$ in Eq. (4).

To simplify our following calculation, we prefer to rewrite Eqs. (1)–(4) in dimensionless forms by introducing dimensionless variables $\bar{x} = k_Lx$, $\bar{t} = 2E_{k_L}t/\hbar$, $\bar{k} = k/k_L$, $\bar{\psi} = \psi/\sqrt{n_0}$, $\bar{g} = gn_0/2E_{k_L}$, $\bar{R} = Rn_0/2E_{k_L}$, $\bar{\gamma}_C = \hbar\gamma_C/2E_{k_L}$, $\bar{\gamma}_R = \hbar\gamma R/2E_{k_L}$, $\bar{\alpha} = \alpha/(2k_LE_{k_L})$, $\bar{P} = \hbar P/2E_{k_L}$, $v = V_0/2E_{k_L}$, and $\bar{n}_R^0 = \bar{\gamma}_C/\bar{R}$ (replacing $\bar{x}$ by x, etc.). Then, by substituting Eqs. (3) and (4) to Eqs. (1) and (2) and only collecting the coefficients of $e^{i\bar{k}x}$ and $e^{i(\bar{k}-1)x}$ for Eq. (1) and e^{ix} and e^{-ix} of Eq. (2) similar to Refs. [2–5], we can obtain an extended nonequilibrium LZ model as follows:

$$i\frac{\partial}{\partial t}\begin{pmatrix} a \\ b \\ u \end{pmatrix} = \begin{pmatrix} L(k) + \bar{g}(|a|^2 + 2|b|^2) & \frac{v}{2} & (\bar{g}_R + \frac{i}{2}\bar{R})b \\ \frac{v}{2} & L(k-1) + \bar{g}(2|a|^2 + |b|^2) & (\bar{g}_R + \frac{i}{2}\bar{R})a \\ -\frac{i\bar{R}\bar{n}_R^0 b^*}{2} & -\frac{i\bar{R}\bar{n}_R^0 a^*}{2} & -i[\bar{\gamma}_R + \bar{R}(|b|^2 + |a|^2)] \end{pmatrix}\begin{pmatrix} a \\ b \\ u \end{pmatrix}, \tag{5}$$

with

$$L(k) = \frac{1}{2}(k - \bar{\alpha}t)^2 + \bar{g}_R\bar{n}_R^0 + \frac{i}{2}(\bar{R}\bar{n}_R^0 - \bar{\gamma}_C). \tag{6}$$

Equation (5) is the central result of this work, which describes the LZ model [i.e., Eq. (5)] for an intrinsically nonequilibrium quantum system with coherent and dissipative dynamics occurring on an equal footing. We also remark that, to our best knowledge, the nonequilibrium LZ problem described by Eq. (5) is investigated for the first time in the context of the polariton condensate.

To illustrate our model based on Eq. (5) the analogies to and differences from the pure LZ model in Refs. [2–5], we first briefly demonstrate how Eq. (5) can be simplified into the pure LZ model in the limiting case corresponding to $u = 0$, $\bar{\gamma}_C = 0$, $\bar{R} = 0$, and $\bar{g}_R = 0$. Here, we are interested in the adiabatic approach by taking $\bar{\alpha}$ a small value. After only keeping the linear term of $\bar{\alpha}$ in Eq. (5), we can arrive at the nonlinear LZ model [4,5] as follows:

$$i\frac{\partial}{\partial t}\begin{pmatrix} a \\ b \end{pmatrix} = \begin{pmatrix} -\bar{\alpha}t + H_{\rm int} & \frac{v}{2} \\ \frac{v}{2} & \bar{\alpha}t - H_{\rm int} \end{pmatrix}\begin{pmatrix} a \\ b \end{pmatrix}, \tag{7}$$

with $H_{\rm int} = \bar{g}(|b|^2 - |a|^2)$. For convenience, we have dropped out the average of the diagonal elements because it does not affect the evolution of the probabilities. The total probability $|a|^2 + |b|^2$ is conserved and is set to be 1. If we further let $\bar{g} = 0$ in Eq. (7), the nonlinear LZ model will become the pure LZ model as is expected [2,3]:

$$i\frac{\partial}{\partial t}\begin{pmatrix} a \\ b \end{pmatrix} = \begin{pmatrix} -\bar{\alpha}t & \frac{v}{2} \\ \frac{v}{2} & \bar{\alpha}t \end{pmatrix}\begin{pmatrix} a \\ b \end{pmatrix}. \tag{8}$$

Before investigating the effects of the nonequilibrium nature on the LZ problem, we first briefly review some important features of a pure LZ model in Eq. (8) and nonlinear LZ model in Eq. (7). As shown by Eqs. (7) and (8). the dynamics of the LZ model are restricted to two quantum states coupled with a constant tunneling matrix element characterized by v. A control parameter labeled by α is swept through the avoided level crossing at a constant velocity. The key quantity of the LZ problem is to calculate the final occupation probability of the two states. There, an exact result of a transition probability r_0 exists for a pure LZ model in Eq. (8), which vanishes exponentially in the adiabatic limit of $\bar{\alpha} \to 0$ as $r_0 = \exp(-\pi v/\bar{\alpha})$ [2,3]. Compared with a pure LZ model in Eq. (8), the most striking feature exhibited by the nonlinear LZ model in Eq. (7) is the presence of a nonzero tunneling probability of r_0 in the adiabatic for the introduction of the interaction term of $H_{\rm int}$ [4,5].

We emphasize that in both cases of pure LZ and nonlinear LZ, the total density labeled by $|a(t)|^2 + |b(t)|^2 = 1$ is a conserved quantity, i.e., $d(|a(t)|^2 + |b(t)|^2)/dt = 0$. In high contrast, with considering the existence of an intrinsically nonequilibrium nature, the probability of $|a(t)|^2 + |b(t)|^2$ immediately becomes a nonconserved quantity, representing the key physics of the nonequilibrium nature affecting the LZ problem.

III. STEADY STATES OF NONEQUILIBRIUM LANDAU-ZENER MODEL

As mentioned in Sec. II, both the pure LZ and nonlinear LZ transitions are referred to as the coherent dynamical problems characterized with the total density of $|a|^2 + |b|^2$ being conserved. Fundamentally, the conserved total density is immediately violated [i.e., $d(|a|^2 + |b|^2)/dt \neq 0$] for the introduction of the dissipation as shown in Eq. (5). Lacking the total conserved density brings the difficulty of defining the tunneling probability properly. For defining the tunneling probability, our strategy is to take the value of a (or b) in the limit of a long time with $a_\infty = \lim_{t\to\infty} a(t)$, which becomes time independent, by solving the equations of motion of Eq. (5). The goal of this section is to check whether there always exist the stationary states of our model in the considered parameter regimes. Note that the key role of the parameter of α in Eq. (1) is to induce the nonadiabatic transitions at avoided level crossings, which does not affect the properties of stationary states. To this end, we are limited to the case of $\alpha = 0$ in Eq. (5) and investigate the long-time behavior of a (or b) by numerically solving Eq. (5) with different initial conditions.

We first choose the case of vanishing periodic strength $v = 0$ and check whether our numerical results can recover the previous well-known results as a test of the validity of our numerical method. As is illustrated in Figs. 1(a1) and 1(b1), for the case of the periodic potential strength $v = 0$, the fluctuation of the reservoir can be set to zero, and the system can evolve into a stationary state where two components are the same no matter $\bar{\gamma}_R < \bar{\gamma}_C$ or $\bar{\gamma}_R > \bar{\gamma}_C$. With vanishing periodic strength $v = 0$, the reservoir density can be immediately calculated as $\bar{n}_R^0 = \bar{P}/(\bar{\gamma}_R + \bar{R}|\psi|^2)$. By plugging $\bar{n}_R^0$ into Eq. (5), the nonequilibrium LZ model of Eq. (5) can be regarded as a two-level system for the ground and first excited states, which is immediately related to Bloch mode dispersions of the p, σ, and π bands in Ref. [44].

Then, we proceed to consider how the periodic potential affects the stationary states by introducing $v \neq 0$. From Figs. 1(b1) and 1(b2), we can find that the population of two-component BECs can be different when the strength of v increases and the fluctuation of the reservoir is stable and nonzero. When $v/2$ is close to $\bar{g}$, occupation of each double well decreases and the fluctuation of reservoir changes with time and the occupation of the polaritons becomes unstable in Fig. 1(c1) with $\bar{\gamma}_C < \bar{\gamma}_R$, while in Fig. 1(c2) the occupation decreases even linearly with time and the fluctuation can still be stable. Finally, occupation of each well decreases with the change of fluctuation $|u|$; that procedure can keep a very long time as shown in Figs. 1(d1) and 1(d2), while the fluctuation of reservoir becomes an oscillating function and vibrates in a high speed [13]. The occupation in two wells will oscillate and decrease when $v/2 > \bar{g}$; these phenomena have been observed in recent experiments [36,38].

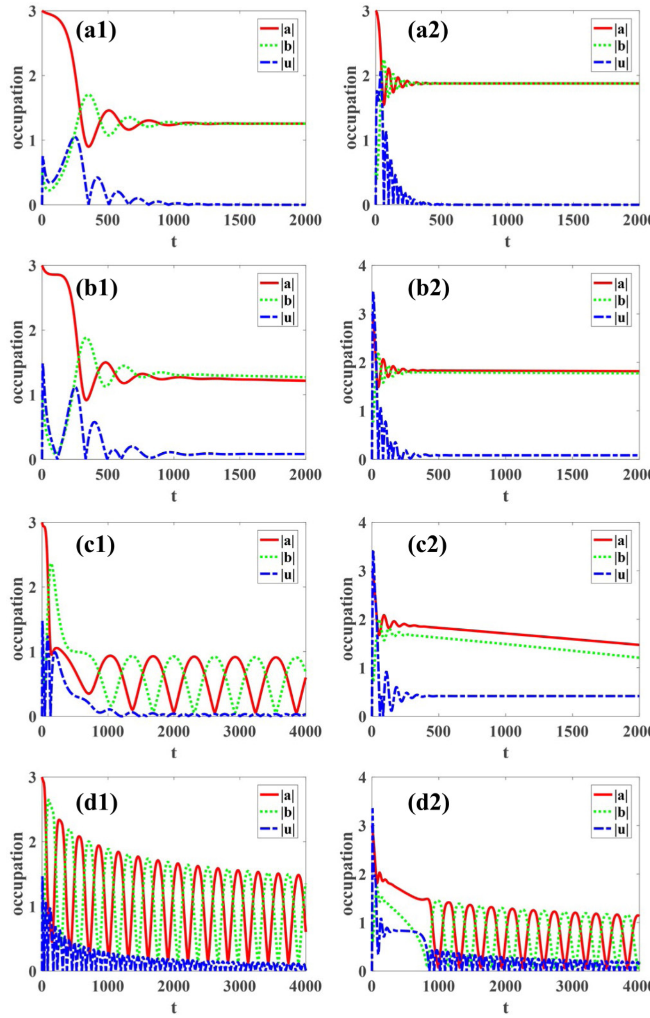

FIG. 1. Nonlinear dynamics of the Bloch mode's amplitudes governed by Eq. (5) with time t (in units of $\hbar/2E_{k_L}$). Dimensionless parameters in Eq. (5) are used: $\bar{\alpha} = 0$, $\bar{\gamma}_C = 0.33$, $\bar{P} = 35$, $\bar{g} = 0.006$, $\bar{g}_R = 2\bar{g}$, $\bar{R} = 0.01$, the first column $\bar{\gamma}_R = 0.495$, the second column $\bar{\gamma}_R = 0.1$, and (a1) and (a2): $v = 0$; (b1) and (b2): $v = 0.002$; (c1) and (c2): $v = 0.01$; (d1) and (d2): $v = 0.02$.

The long-time-independent stationary states in Fig. 1 can be explained by calculating the time variation of the total density probability of the condensate density with the help of Eq. (5) as

$$\frac{d}{dt}(|a|^2 + |b|^2) = \bar{R}u(a^*b + b^*a). \tag{9}$$

From Eq. (9), the condition of the total density probability being conserved depends on two parameters: the fluctuation of reservoir u and the relative phase between a and b. In such, there are three possible cases under which the total density probability still is a conserved quantity even with dissipation.

Case 1. $u = 0$, which indicates the fluctuation of reservoir is zero. This corresponds to the case that the reservoir is too large to be influenced by the polariton condensate.

Case 2. $|a|$ or $|b|$ is zero. This means the polariton condensate is willing to stay in one mode of the two-mode approximation.

Case 3. The relative phase between a and b are fixed to be $\theta_a - \theta_b = \frac{\pi}{2} + j\pi$ with j being an integer.

In what follows, we plan to double check above three possible cases of the total density probability still being a conserved quantity even with dissipation. First, it's physically reasonable that the system should be stable in the case of u being a very small quantity compared to the reservoir density of n_R^0, although the total density probability is not the conserved quantity any more according to Eq. (9) as shown in Fig. 1. According to Eq. (2), we can obtain the steady value of the reservoir as follows:

$$\bar{n}_R^0 = \frac{\bar{P}}{\bar{\gamma}_R + \bar{R}|\psi|^2} \approx \frac{\bar{P}}{\bar{\gamma}_R}\left(1 - \frac{R}{\bar{\gamma}_R}|\psi|^2\right), \tag{10}$$

for $\bar{R} \ll \bar{\gamma}_R$. By substituting it to Eq. (5) as done in Ref. [36], we can obtain the analytical expression of u:

$$u = -\bar{R}\bar{n}_R^0 \frac{ab^* + a^*b}{2\bar{\gamma}_{\bar{R}} + 2\bar{R}(|b|^2 + |a|^2)}. \tag{11}$$

The time-dependent dynamics of condensate density due to Eq. (9) becomes

$$\frac{dn}{dt} = -\bar{R}^2\bar{n}_R^0 \frac{(ab^* + a^*b)^2}{2\gamma_{\bar{R}} + 2\bar{R}(|b|^2 + |a|^2)}, \tag{12}$$

which makes the physics of Eq. (9) clearer. By Eq. (12), the total density can be conserved by choosing u, a, or b to be zero corresponding to Case one and Case two, respectively. The special relative phases between parameters of a and b can also stabilize the system corresponding to Case three.

We are limited ourselves to the case of the reservoir having a steady value as is shown in Figs. 1(a1)–1(c1) and 1(b2)–1(c2). Within these parameter regimes, we substitute the form of u to Eq. (5). After dropping an energy shift of $E_{\text{shift}} = 1/8 + \bar{g}_R\bar{n}_R^0$ with $\bar{n}_R^0 = \bar{\gamma}_C/\bar{R}$, we can rewrite our model of Eq. (5) into the following form:

$$i\frac{\partial}{\partial t}\begin{pmatrix} a \\ b \end{pmatrix} = \begin{pmatrix} \bar{g}(2|b|^2 + |a|^2) - (\lambda + i\chi)|b|^2 - \gamma/2 & v/2 - (\lambda + i\chi)a^*b \\ v/2 - (\lambda + i\chi)b^*a & \bar{g}(2|a|^2 + |b|^2) - (\lambda + i\chi)|a|^2 + \gamma/2 \end{pmatrix}\begin{pmatrix} a \\ b \end{pmatrix}, \tag{13}$$

with $(\lambda + i\chi) = \frac{(\bar{g}_R + \frac{i}{2}\bar{R})\bar{R}\bar{n}_R^0}{2\bar{\gamma}_R + 2\bar{R}n}$. Equation (13) is an effective version of nonequilibrium LZ model of Eq. (7) proposed in this work.

Above, we have developed the analytically physical picture and predicted features of the total density probability still being a conserved quantity even with dissipation. Below, we are interested in how the relative phase of two Bloch modes can stabilize total density probability by numerically solving Eq. (5). We choose the parameter regimes with total density probability being conserved and plot the corresponding relative phase of two Bloch modes in Fig. 2. It's clear now that the relative phase changes between $-\pi/2$ and $3\pi/2$ [see Fig. 2(a1)] in the weak pumping region. This suggests that the relative phases are oscillating around $\pi/2 + j\pi$ consistent with the prediction of Eq. (9). In contrast, in Fig. 1(c2) and Fig. 2(b2) the population of polaritons cannot reach a balance in the strong pumping region ($\bar{\gamma}_R < \bar{\gamma}_C$), because the imaginary part of elementary excitation can be larger than zero and the relative phase is not exactly between $-3\pi/2$ and $\pi/2$, but it is also a stable relative phase leading to linear decay. Our numerical results can also explain partly the results of Ref. [36], where authors have observed a smoothed sawtooth phase evolution with a much smaller amplitude (-0.3π to 0.3π). This result is very close to -0.5π and 0.5π in our theory and the profile of population changing with time is also consistent with ours.

IV. NONEQUILIBRIUM LANDAU-ZENER TUNNELING

Before analyzing the nonequilibrium LZ problem, it is essential to establish that the model system itself described by Eqs. (1) and (2) is stable with respect to weak perturbations [13]. In more detail, one would introduce perturbations to a steady state and solve the corresponding Bogoliubov–de Gennes (BdG) equations [14]. If the imaginary part of the excitation spectrum leads to an exponential decay for the perturbation amplitude, then the original steady state can be considered as stable against such perturbation. In this work, we limit ourselves into the modulationally stable parameter regimes [13]. Meanwhile, we also numerically double check that the dynamics of the polariton condensate described by the nonequilibrium LZ model of Eq. (5) are always dynamically stable.

In this section, we will pay attention to the adiabatic process by evolving a state from $t = -\infty$ to ∞ numerically. There is lots of work that has been done in adiabatic theory [4,5,63,64], but for the polariton system, there are some new results. In the past, the initial state is set to the lower state and the upper state can be calculated as tunneling probability for the conserved population, however, it is difficult to define the tunneling opportunity in an open system. We focus on the occupation of each state before and after tunneling for the atom loss of the system. Considering the linear of t for Hamiltonian is dependent on time and changes slowly in a nonlinear polariton system. In Sec. III, we investigate the occupation of each state will oscillate and decrease when v is large enough. More details about tunneling will be discussed in this section.

As is vividly shown in Fig. 3, we evolute the initial state from $(a, b, u) = (0, \sqrt{\bar{P}/\bar{\gamma}_C - \bar{\gamma}_R/\bar{R}}, 0)$ and find the fluctuation has a sudden change at $t = 0$ from zero to nonzero. Two levels will have a crossover near $t = 0$ and the initial occupation will vanish when $t > 0$ for the fluctuation of the reservoir. Comparing Figs. 3(a1) and 3(b1) with Figs. 3(a2) and 3(b2), the peak of fluctuation in the weak pumping region ($\bar{\gamma}_R > \bar{\gamma}_C$) is lower than that in the strong pumping region ($\bar{\gamma}_R < \bar{\gamma}_C$). We can also find that larger depth of periodic

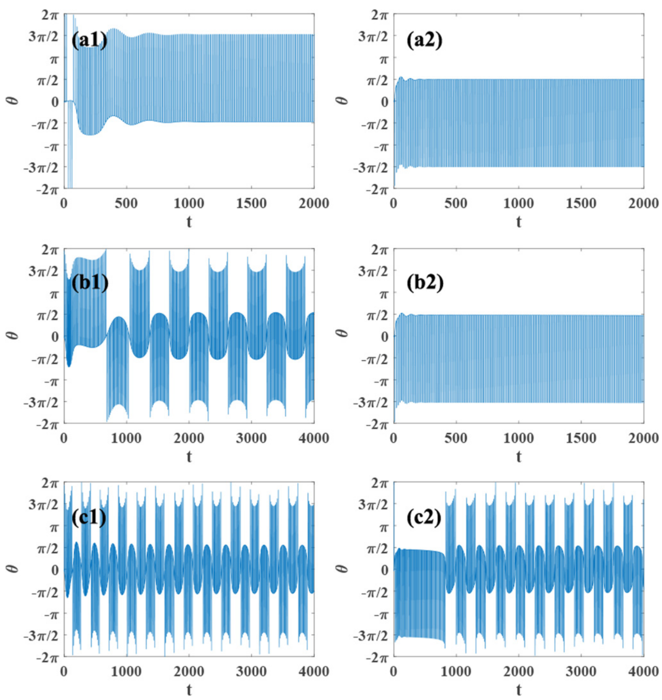

FIG. 2. Nonlinear dynamics of the Bloch mode's relative phase $\theta = \theta_b - \theta_a$ governed by Eq. (5) with time t (in units of $\hbar/2E_{k_L}$). Dimensionless parameters in Eq. (5) are used: $\bar{\alpha} = 0$, $\bar{\gamma}_C = 0.33$, $\bar{P} = 35$, $\bar{g} = 0.006$, $\bar{g}_R = 2\bar{g}$, $\bar{R} = 0.01$, the left column $\bar{\gamma}_R = 0.495$, the right column $\bar{\gamma}_R = 0.1$, and (a1) and (a2): $v = 0.002$; (b1) and (b2): $v = 0.01$; (c1) and (c2): $v = 0.02$.

potential can reduce more occupation in the final states after tunneling as is shown $v = 0.02$ in Fig. 3(b1) compared to $v = 0.002$ in Fig. 3(a1) if we fix interaction strength. If it is a double-well system to study the Josephson junction between two wells, the oscillations have a short lifetime as particle

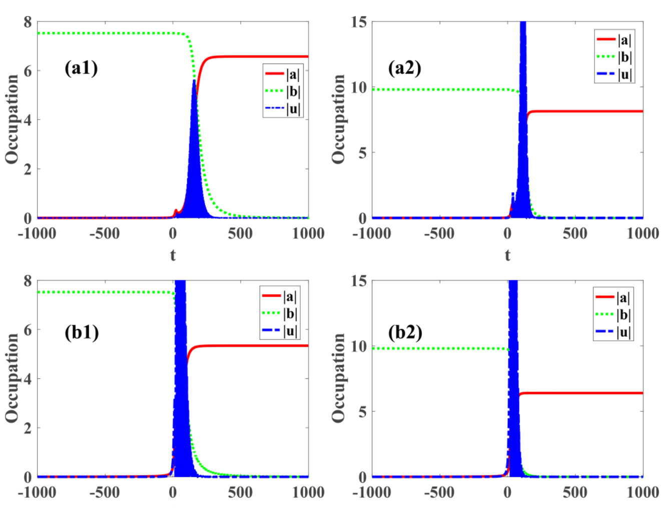

FIG. 3. Numerical results for the time evolution of Eq. (5) with the time t (in unit of $\hbar/2E_{k_L}$). Dimensionless parameters in Eq. (5) are used: $\bar{g} = 0.006$, $\bar{\alpha} = 0.02$, $\bar{g}_R = 2\bar{g}$, $\bar{P} = 35$, $\bar{\gamma}_C = 0.33$, $\bar{R} = 0.01$; (a1): $\bar{v} = 0.002$, $\bar{\gamma}_R = 0.495$; (b1): $v = 0.002$, $\bar{\gamma}_R = 0.1$; (a2): $v = 0.02$, $\bar{\gamma}_R = 0.495$; and (b2): $v = 0.02$, $\bar{\gamma}_R = 0.1$.

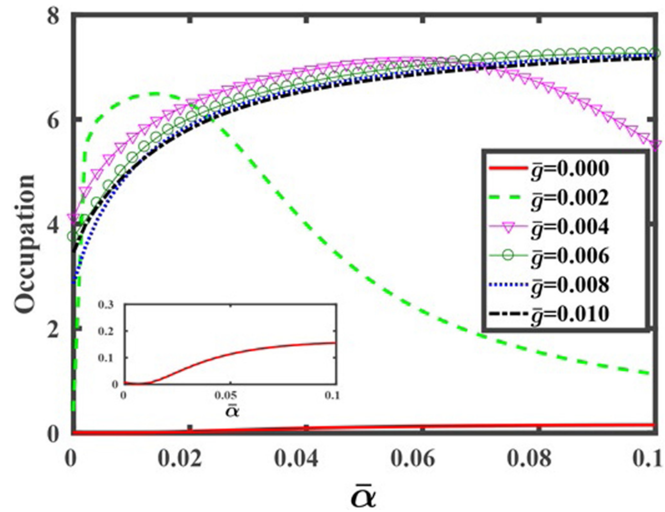

FIG. 4. Numerical results for the tunneling occupation as a function of $\bar{\alpha}$ by solving Eq. (5) with the initial states $(a, b, u) = (0, \sqrt{\bar{P}/\bar{\gamma}_C - \bar{\gamma}_R/\bar{R}}, 0)$. Dimensionless parameters in Eq. (5) are used: $\bar{g}_R = 2\bar{g}$, $\bar{P} = 35$, $\bar{\gamma}_C g = 0.33$, $\bar{\gamma}_R = 0.495$, $\bar{R} = 0.01$, and $v = 0.01$.

number decreases after tunneling if the temperature is beyond zero ($\bar{\alpha} > 0$).

It is known that interaction strength g can change the tunneling probability from zero to a finite value for an adiabatic evolution, and it will break down the Bloch oscillation. In recent experiments, the interaction of polariton can be adjusted by Feshbach resonance [35], so we can use the numerical calculation to find the rule of tunneling occupation along with adiabatic coefficients. The inset in Fig. 4 is the enlarged drawing of the condition $\bar{g} = 0$, and we can see the branch point is off the real axis leading to a transition occupation vanishing exponentially in the adiabatic limit [4,5]. The result is completely according to the close system for which we set $\bar{g}_R = 2\bar{g}$, and there is no interaction between the reservoir and the polaritons, but the dissipative $\bar{\gamma}_C$ leads to the particle loss. Here, we just consider $\bar{P} \gg \bar{P}_{\text{th}}$ in Fig. 4. When interaction $\bar{g}$ is beyond zero, occupation after tunneling will decrease after reaching a peak for the fluctuation of the reservoir, which is a result of competition between LZ driving and relaxation [65–68]. Besides, the increase of nonlinear interaction between the reservoir and polaritons makes the system stable again, which leads to dynamical stability even though the acceleration $\bar{\alpha}$ is much larger. The competition between dissipative coefficients and the nonlinear interaction of reservoir and polaritons bring a powerful tool to achieve a new equilibrium.

V. THE MOTION OF HAMILTONIAN IN PHASE SPACE

In this section, we focus on the motions of the polariton system in phase space. Here, we consider two components $a = ae^{i\theta_a}$, $b = be^{i\theta_b}$, population difference $s = |b|^2 - |a|^2$, total population $n = |b|^2 + |a|^2$, the relative phase $\theta = \theta_b - \theta_a$, and the product of two components $|ab| = \sqrt{n^2 - s^2}/2$.

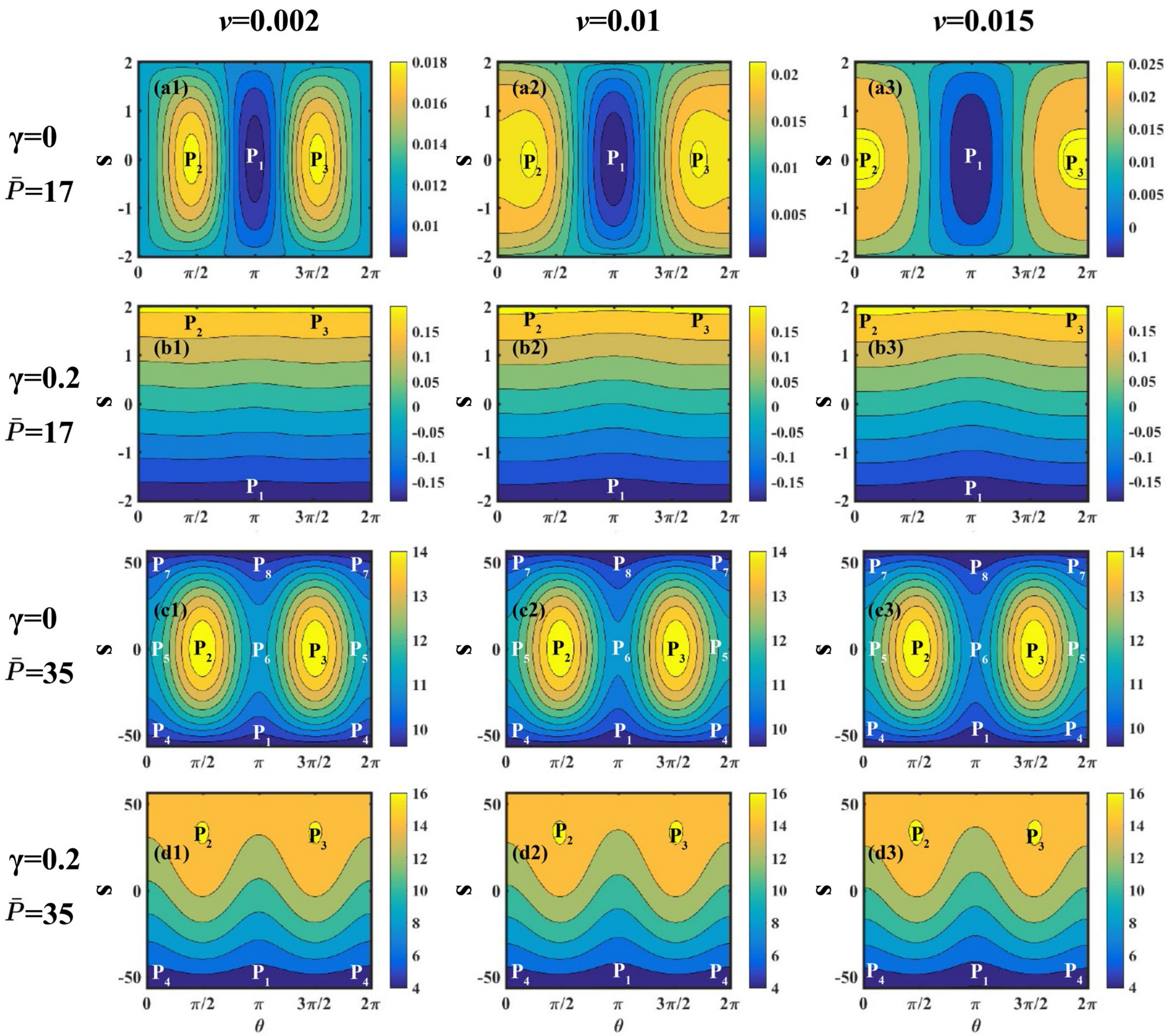

FIG. 5. Evolution of the phase space motions of Hamiltonian (14) in phase space (s, θ). Dimensionless parameters in Eq. (14) are used: $\bar{g} = 0.006$, $\bar{\gamma}_R = 0.496$, $\bar{\gamma}_C = 0.33$, $\bar{R} = 0.01$, $\bar{g}_R = 2\bar{g}$. The fixed points P_2 and P_3 will move from the relative phase $\pi/2$ and $3\pi/2$ to 0 and 2π along with the increase of the periodic strength v. Besides, more fixed points will appear if the pumping rate $\bar{P}$ is large enough, and some fixed points will vanish because of the existence of adiabatic parameter γ.

From Eq. (13), the total energy of the system can be cast into an effective Hamiltonian [69,70]:

$$E = \bar{g}\frac{3n^2 - s^2}{4} + \gamma s/2 + v\cos\theta\sqrt{n^2 - s^2}/2 - (\lambda + i\chi)\frac{n^2 - s^2}{2}\cos^2\theta, \tag{14}$$

with $\gamma = \bar{\alpha}t$. The energy is only corresponding to n, s, θ and the imaginary part of E is always a periodic function to θ, so we only consider the real part. The fixed points of the effective Hamiltonian correspond to the eigenstates of the nonlinear two-level system and the extreme points require

$$\frac{\partial}{\partial\theta}E = (n^2 - s^2)\lambda\sin 2\theta - \frac{\sqrt{n^2 - s^2}}{2}v\sin\theta, \tag{15}$$

$$\frac{\partial}{\partial s}E = \frac{\gamma}{2} - \frac{\bar{g}s}{2} + 2\lambda s\cos^2\theta - \frac{sv\cos\theta}{2\sqrt{n^2 - s^2}}, \tag{16}$$

$$\frac{\partial}{\partial n}E = \frac{3\bar{g}n}{2} + \frac{nv\cos\theta}{2\sqrt{n^2 - s^2}} - \cos^2\theta\left[2\lambda n + (n^2 - s^2)\frac{d\lambda}{dn}\right], \tag{17}$$

with $\frac{d}{dn}\lambda = -\frac{\bar{g}_R\bar{R}^2\bar{n}_R^0}{2(\bar{\gamma}_R + \bar{R}n)^2}$. From Eq. (15), the fixed points only appear when $\sin\theta = 0$ or $s = \pm n$, or $\cos\theta = \frac{v}{4\lambda\sqrt{n^2 - s^2}}$. The solution is $s = \pm n$, or $\theta = 0, \pi$ or $\theta = \arccos\left(\frac{v}{4\lambda\sqrt{n^2-s^2}}\right)$. Here we have a new solution if $\left|\frac{v}{4\lambda\sqrt{n^2-s^2}}\right| \leqslant 1$ and n represents the density of polariton, so it must be a positive number and can be controlled by pump rate $\bar{P}$.

First, we want to focus on the pumping rate that is near the threshold $\bar{P}_{\rm th}$ and how the adiabatic process influences the phase space of the system. As is shown in Figs. 5(a1)–5(a3), there are only three fixed points: one is at $\theta = \pi$ and the others appear near $\theta = \pi/2$ and $\theta = 3\pi/2$, along with the increase of v; fixed points go to the border of the phase at the adiabatic process with $\gamma = 0$. In Fig. 5(a3) fixed points P_2 and P_3 are the same. When γ is beyond zero, fixed point P_1 goes to the border $s = -n$ and points P_2 and P_3 go to the border $s = n$ as is shown in Figs. 5(b1)–5(b3).

The polariton system's particle number can be adjusted by pumping rate and if we set $\bar{P} \gg \bar{P}_{\rm th}$, the system will have different results. There are eight fixed points in phase space: P_1, P_6, and P_8 appear at $\theta = \pi$, meanwhile, P_2 and P_3 appear at $\theta = \pi/2$ and $3\pi/2$ and other points appear at $\theta = 0$ as is shown in Figs. 5(c1)–5(c3). Point P_5 or point P_6 is the saddle point and can annihilate itself by colliding with P_1 as R changes slowly, leading to the breakdown of adiabaticity of the tunneling [70]. Furthermore, P_5 and P_6 will also annihilate with P_4 and P_1, so in this situation, there may be two loops at $k = 1/2$ as are reported in Ref. [43]. There are two saddle points when $v/2 < g$, because we need to compare gn with $v/2$ and in our region $\bar{g}n \gg v/2$ for $\bar{P} \gg \bar{P}_{\rm th}$.

VI. CONCLUSION

In summary, we obtain and study the nonequilibrium LZ model of the polariton condensate in a periodic potential under nonresonant pumping by the two-mode approximation to the driven-dissipative GP equations coupled to a rate equation for the reservoir density. In the past, the fluctuations of the reservoir are routine and not under consideration for they are much smaller than the reservoir, but they play a very important role in the tunneling process. The steady states of the system provide that the relative phase can only be $\pi/2 + j\pi$ in the Josephson junction, and atoms will lose after tunneling for fluctuations has a sudden peak near $t = 0$. The numerical results of the tunneling process agree with Ref. [36] very well. If we set the fluctuation of the reservoir to a constant, the simplified model is similar to the model discussed in Ref. [44]. Last but not least, the motion of the Hamiltonian in phase space reveals two loops in the band structure, which is obtained in Ref. [43] with different methods.

ACKNOWLEDGMENTS

We thank Y. Xue, Ying Hu, J. Liu, and B. Wu for stimulating discussions. This is supported by the National Natural Science Foundation of China (Grant No. 11604300) and Key Projects of the Natural Science Foundation of China (Grant No. 11835011). Z.D.Z. is supported by the NSFC of China (Grant No. 51331006).

[1] N. V. Vitanov, A. A. Rangelov, B. W. Shore, and K. Bergmann, Stimulated raman adiabatic passage in physics, chemistry, and beyond, Rev. Mod. Phys. **89**, 015006 (2017).

[2] L. D. Laudau, Zur theorie der energie Übertragung ii, Phys. Z. Sowjet **2**, 56 (1932).

[3] C. Zener and R. H. Fowler, Non-adiabatic crossing of energy levels, Proc. R. Soc. Lond. **137**, 696 (1932).

[4] B. Wu and Q. Niu, Nonlinear Landau-Zener tunneling, Phys. Rev. A **61**, 023402 (2000).

[5] B. Wu and Q. Niu, Superfluidity of Bose-Einstein condensate in an optical lattice: Landau-Czener tunneling and dynamical instability, New J. Phys. **5**, 104 (2003).

[6] I. Bloch, J. Dalibard, and W. Zwerger, Many-body physics with ultracold gases, Rev. Mod. Phys. **80**, 885 (2008).

[7] O. Morsch and M. Oberthaler, Dynamics of Bose-Einstein condensates in optical lattices, Rev. Mod. Phys. **78**, 179 (2006).

[8] I. Carusotto and C. Ciuti, Quantum fluids of light, Rev. Mod. Phys. **85**, 299 (2013).

[9] I. A. Shelykh, A. V. Kavokin, Y. G. Rubo, T. C. H. Liew, and G. Malpuech, Polariton polarization-sensitive phenomena in planar semiconductor microcavities, Semicond. Sci. Technol. **25**, 013001 (2010).

[10] H. Deng, H. Haug, and Y. Yamamoto, Exciton-polariton Bose-Einstein condensation, Rev. Mod. Phys. **82**, 1489 (2010).

[11] J. Keeling and N. G. Berloff, Exciton-polariton condensation, Contemp. Phys. **52**, 131 (2011).

[12] T. Byrnes, N. Y. Kim, and Y. Yamamoto, Exciton-polariton condensates, Nat. Phys. **10**, 803 (2014).

[13] M. Wouters and I. Carusotto, Excitations in a Nonequilibrium Bose-Einstein Condensate of Exciton Polaritons, Phys. Rev. Lett. **99**, 140402 (2007).

[14] X. Xu, Y. Hu, Z. Zhang, and Z. Liang, Spinor polariton condensates under nonresonant pumping: Steady states and elementary excitations, Phys. Rev. B **96**, 144511 (2017).

[15] K. C. Huang, P. Bienstman, J. D. Joannopoulos, K. A. Nelson, and S. Fan, Phonon-polariton excitations in photonic crystals, Phys. Rev. B **68**, 075209 (2003).

[16] O. Kyriienko and I. A. Shelykh, Elementary excitations in spinor polariton-electron systems, Phys. Rev. B **84**, 125313 (2011).

[17] M. Wouters and I. Carusotto, Probing the excitation spectrum of polariton condensates, Phys. Rev. B **79**, 125311 (2009).

[18] S. S. Gavrilov, A. V. Sekretenko, S. I. Novikov, C. Schneider, S. Hofling, M. Kamp, A. Forchel, and V. D. Kulakovskii, Polariton multistability and fast linear-to-circular polarization conversion in planar microcavities with lowered symmetry, Appl. Phys. Lett. **102**, 011104 (2013).

[19] N. Takemura, S. Trebaol, M. Wouters, M. T. Portella-Oberli, and B. Deveaud, Heterodyne spectroscopy of polariton spinor interactions, Phys. Rev. B **90**, 195307 (2014).

[20] Y.-C. Zhang, X.-F. Zhou, G.-C. Guo, X. Zhou, H. Pu, and Z.-W. Zhou, Two-component polariton condensate in an optical microcavity, Phys. Rev. A **89**, 053624 (2014).

[21] J. Wang, W. Xie, L. Zhang, D. Xu, W. Liu, J. Lu, Y. Wang, J. Gu, Y. Chen, X. Shen, and Z. Chen, Exciton-polariton condensate induced by evaporative cooling in a three-dimensionally confined microcavity, Phys. Rev. B **91**, 165423 (2015).

[22] S. Utsunomiya, L. Tian, G. Roumpos, C. W. Lai, N. Kumada, T. Fujisawa, M. Kuwata-Gonokami, A. Loffler, S. Höfling, A. Forchel, and Y. Yamamoto, Observation of Bogoliubov excitations in exciton-polariton condensates, Nat. Phys. **4**, 700 (2008).
[23] M. Aßmann, J.-S. Tempel, F. Veit, M. Bayer, A. Rahimi-Iman, A. Löffler, S. Höfling, S. Reitzenstein, L. Worschech, and A. Forchel, From polariton condensates to highly photonic quantum degenerate states of bosonic matter, Proc. Natl. Acad. Sci. USA **108**, 1804 (2011).
[24] Y. Wang, T. Hu, W. Xie, L. Sun, L. Zhang, J. Wang, J. Gu, L. Wu, J. Wang, X. Shen, and Z. Chen, Polarization-coupled polariton pairs in a birefringent microcavity, Phys. Rev. B **91**, 121301(R) (2015).
[25] M. Sich, D. N. Krizhanovskii, M. S. Skolnick, A. V. Gorbach, R. Hartley, D. V. Skryabin, E. A. Cerda-Méndez, K. Biermann, R. Hey, and P. V. Santos, Observation of bright polariton solitons in a semiconductor microcavity, Nat. Photon. **6**, 50 (2011).
[26] E. A. Ostrovskaya, J. Abdullaev, M. D. Fraser, A. S. Desyatnikov, and Y. S. Kivshar, Self-localization of Polariton Condensates in Periodic Potentials, Phys. Rev. Lett. **110**, 170407 (2013).
[27] F. Pinsker and H. Flayac, Bright solitons in non-equilibrium coherent quantum matter, Proc. R. Soc. London, Ser. A **472**, 20150592 (2016).
[28] G. Grosso, G. Nardin, F. Morier-Genoud, Y. Léger, and B. Deveaud-Plédran, Dynamics of dark-soliton formation in a polariton quantum fluid, Phys. Rev. B **86**, 020509(R) (2012).
[29] A. Amo, S. Pigeon, D. Sanvitto, V. G. Sala, R. Hivet, I. Carusotto, F. Pisanello, G. Leménager, R. Houdré, E Giacobino, C. Ciuti, and A. Bramati, Polariton superfluids reveal quantum hydrodynamic solitons, Science **332**, 1167 (2011).
[30] Y. Xue and M. Matuszewski, Creation and Abrupt Decay of a Quasistationary Dark Soliton in a Polariton Condensate, Phys. Rev. Lett. **112**, 216401 (2014).
[31] L. A. Smirnov, D. A. Smirnova, E. A. Ostrovskaya, and Y. S. Kivshar, Dynamics and stability of dark solitons in exciton-polariton condensates, Phys. Rev. B **89**, 235310 (2014).
[32] X. Xu, L. Chen, Z. Zhang, and Z. Liang, Dark-bright solitons in spinor polariton condensates under nonresonant pumping, J. Phys. B: At., Mol. Opt. Phys. **52**, 025303 (2018).
[33] F. Pinsker, Approximate solutions for half-dark solitons in spinor non-equilibrium polariton condensates, Ann. Phys. **362**, 726 (2015).
[34] M. Vladimirova, S. Cronenberger, D. Scalbert, K. V. Kavokin, A. Miard, A. Lemaître, J. Bloch, D. Solnyshkov, G. Malpuech, and A. V. Kavokin, Polariton-polariton interaction constants in microcavities, Phys. Rev. B **82**, 075301 (2010).
[35] N. Takemura, S. Trebaol, M. Wouters, M. T. Portella-Oberli, and B. Deveaud, Polaritonic Feshbach resonance, Nat. Phys. **10**, 500 (2014).
[36] K. G. Lagoudakis, B. Pietka, M. Wouters, R. André, and B. Deveaud-Plédran, Coherent Oscillations in an Exciton-Polariton Josephson Junction, Phys. Rev. Lett. **105**, 120403 (2010).
[37] M. Abbarchi, A. Amo, V. G. Sala, D. D. Solnyshkov, H. Flayac, L. Ferrier, I. Sagnes, E. Galopin, A. Lemaître, G. Malpuech, and J. Bloch, Macroscopic quantum self-trapping and Josephson oscillations of exciton polaritons, Nat. Phys. **9**, 275 (2013).
[38] G. Pavlovic, G. Malpuech, and I. A. Shelykh, Pseudospin dynamics in multimode polaritonic Josephson junctions, Phys. Rev. B **87**, 125307 (2013).
[39] S. S. Gavrilov, A. S. Brichkin, S. I. Novikov, S. Höfling, C. Schneider, M. Kamp, A. Forchel, and V. D. Kulakovskii, Nonlinear route to intrinsic Josephson oscillations in spinor cavity-polariton condensates, Phys. Rev. B **90**, 235309 (2014).
[40] C. W. Lai, N. Y. Kim, S. Utsunomiya, G. Roumpos, H. Deng, M. D. Fraser, T. Byrnes, P. Recher, N. Kumada, T. Fujisawa, and Y. Yamamoto, Coherent zero-state and π-state in an exciton–polariton condensate array, Nature (London) **450**, 529 (2007).
[41] E. A. Cerda-Méndez, D. N. Krizhanovskii, K. Biermann, R. Hey, M. S. Skolnick, and P. V. Santos, Wavefunction of polariton condensates in a tunable acoustic lattice, New J. Phys. **14**, 075011 (2012).
[42] D. N. Krizhanovskii, E. A. Cerda-Méndez, S. Gavrilov, D. Sarkar, K. Guda, R. Bradley, P. V. Santos, R. Hey, K. Biermann, M. Sich, F. Fras, and M. S. Skolnick, Effect of polariton-polariton interactions on the excitation spectrum of a nonequilibrium condensate in a periodic potential, Phys. Rev. B **87**, 155423 (2013).
[43] I. Yu. Chestnov, A. V. Yulin, A. P. Alodjants, and O. A. Egorov, Nonlinear Bloch waves and current states of exciton-polariton condensates, Phys. Rev. B **94**, 094306 (2016).
[44] T. Gao, O. A. Egorov, E. Estrecho, K. Winkler, M. Kamp, C. Schneider, S. Höfling, A. G. Truscott, and E. A. Ostrovskaya, Controlled Ordering of Topological Charges in an Exciton-Polariton Chain, Phys. Rev. Lett. **121**, 225302 (2018).
[45] T. Karzig, C.-E. Bardyn, N. H. Lindner, and G. Refael, Topological Polaritons, Phys. Rev. X **5**, 031001 (2015).
[46] A. V. Nalitov, D. D. Solnyshkov, and G. Malpuech, Polariton $\mathbb{Z}$ Topological Insulator, Phys. Rev. Lett. **114**, 116401 (2015).
[47] W. Langbein, I. Shelykh, D. Solnyshkov, G. Malpuech, Y. Rubo, and A. Kavokin, Polarization beats in ballistic propagation of exciton-polaritons in microcavities, Phys. Rev. B **75**, 075323 (2007).
[48] C. Leyder, M. Romanelli, J. Ph. Karr, E. Giacobino, T. C. H. Liew, M. M. Glazov, A. V. Kavokin, G. Malpuech, and A. Bramati, Observation of the optical spin Hall effect, Nat. Phys. **3**, 628 (2007).
[49] M. Biondi, E. P. L. van Nieuwenburg, G. Blatter, S. D. Huber, and S. Schmidt, Incompressible Polaritons in a Flat Band, Phys. Rev. Lett. **115**, 143601 (2015).
[50] D. Leykam and S. Flach, Perspective: Photonic flatbands, APL Photonics **3**, 070901 (2018).
[51] M. Sun, I. G. Savenko, S. Flach, and Y. G. Rubo, Excitation of localized condensates in the flat band of the exciton-polariton Lieb lattice, Phys. Rev. B **98**, 161204(R) (2018).
[52] D. Leykam, A. Andreanov, and S. Flach, Artificial flat band systems: From lattice models to experiments, Adv. Phys: X **3**, 1473052 (2018).
[53] B. Qi, L. Zhang, and L. Ge, Defect states Emerging from a non-Hermitian Flatband of Photonic Zero Modes, Phys. Rev. Lett. **120**, 093901 (2018).
[54] M. M. de Lima and P. V. Santos, Modulation of photonic structures by surface acoustic waves, Rep. Prog. Phys. **68**, 1639 (2005).
[55] S. Endo, T. Oka, and H. Aoki, Tight-binding photonic bands in metallophotonic waveguide networks and flat bands in kagome lattices, Phys. Rev. B **81**, 113104 (2010).

[56] H. Takeda, T. Takashima, and K. Yoshino, Flat photonic bands in two-dimensional photonic crystals with kagome lattices, J. Phys.: Condens. Matter **16**, 6317 (2004).

[57] N. Y. Kim, K. Kusudo, C. Wu, N. Masumoto, A. Löffler, S. Höfling, N. Kumada, L. Worschech, A. Forchel, and Y. Yamamoto, Dynamical d-wave condensation of exciton–polaritons in a two-dimensional square-lattice potential, Nat. Phys. **7**, 681 (2011).

[58] C. Schneider, K. Winkler, M. D. Fraser, M. Kamp, Y. Yamamoto, E. A. Ostrovskaya, and S. Höfling, Exciton-polariton trapping and potential landscape engineering, Rep. Prog. Phys. **80**, 016503 (2016).

[59] Y. Zhang, X. Zhang, B. Tang, C. Tian, C. Xu, H. Dong, and W. Zhou, Realization of an all-optically controlled dynamic superlattice for exciton-polaritons, Nanoscale **10**, 14082 (2018).

[60] K. Winkler, O. A. Egorov, I. G. Savenko, X. Ma, E. Estrecho, T. Gao, S. Müller, M. Kamp, T. C. H. Liew, E. A. Ostrovskaya, S. Höfling, and C. Schneider, Collective state transitions of exciton polaritons loaded into a periodic potential, Phys. Rev. B **93**, 121303(R) (2016).

[61] A. Amo and J. Bloch, Exciton-polaritons in lattices: A nonlinear photonic simulator, C. R. Phys. **17**, 934 (2016).

[62] A. V. Nalitov, T. C. H. Liew, A. V. Kavokin, B. L. Altshuler, and Y. G. Rubo, Spontaneous Polariton Currents in Periodic Lateral Chains, Phys. Rev. Lett. **119**, 067406 (2017).

[63] P. G. Kevrekidis, W. Wang, R. Carretero-González, and D. J. Frantzeskakis, Adiabatic invariant analysis of dark and dark-bright soliton stripes in two-dimensional Bose-Einstein condensates, Phys. Rev. A **97**, 063604 (2018).

[64] N. Bobrovska and M. Matuszewski, Adiabatic approximation and fluctuations in exciton-polariton condensates, Phys. Rev. B **92**, 035311 (2015).

[65] P. Nalbach and M. Thorwart, Landau-Zener Transitions in a Dissipative Environment: Numerically Exact Results, Phys. Rev. Lett. **103**, 220401 (2009).

[66] S. Javanbakht, P. Nalbach, and M. Thorwart, Dissipative Landau-Zener quantum dynamics with transversal and longitudinal noise, Phys. Rev. A **91**, 052103 (2015).

[67] Z. Huang and Y. Zhao, Dynamics of dissipative Landau-Zener transitions, Phys. Rev. A **97**, 013803 (2018).

[68] R. K. Malla and M. E. Raikh, Landau-Zener transition in a two-level system coupled to a single highly excited oscillator, Phys. Rev. B **97**, 035428 (2018).

[69] O. Zobay and B. M. Garraway, Time-dependent tunneling of Bose-Einstein condensates, Phys. Rev. A **61**, 033603 (2000).

[70] J. Liu, B. Wu, and Q. Niu, Nonlinear Evolution of Quantum States in the Adiabatic Regime, Phys. Rev. Lett. **90**, 170404 (2003).